City Research Online

City, University of London Institutional Repository

This is the unspecified version of the paper.

This version of the publication may differ from the final published version.

Link to published version:

Simulation of heating effects in cavitating flows through Diesel fuel injectors caused by extreme fuel pressurisation

Andreas Theodorakakos, Nicholas Mitroglou and Manolis Gavaises*

International Institute for Cavitation Research
School of Engineering and Mathematical Sciences
City University London, UK

*Corresponding author: m.gavaises@city.ac.uk Tel: +44(0)20 7040 8115

ABSTRACT

Pressurization of Diesel fuel in modern common-rail injectors in excess of 2000bar can result to increased temperatures and significant variation of the fuel physical properties (density, viscosity, heat capacity and thermal conductivity) relative to those under atmospheric pressure and room temperature conditions. Moreover, due to the sharp de-pressurization experienced by the fuel at the inlet of the injection holes, significant gradients of the above properties are established. The subsequent fuel acceleration at velocities reaching 700m/s is also inducing further wall friction and thus heating. Consequently, the characteristics of cavitation taking place at the entrance to the injection holes are altered while the volumetric efficiency of the nozzle is significantly affected. The present study quantifies the role of these effects in mini sac-type Diesel injectors operating at pressures up to 2400bar through use of a RANS cavitation CFD model. The flow solver is accordingly modified to account for such effects during the solution of the flow conservation equations. Two different injector designs have been considered, both based on the same mini sac-type nozzle body; one with sharp-inlet cylindrical holes and one with tapered holes with inlet rounding. The results indicate significant changes in terms of the details of the flow development but also to bulk flow characteristics such as the volumetric efficiency of the injectors and the mean fuel injection temperature relative to the isothermal/constant properties case.

Keywords: Cavitation, Diesel injectors, Fuel pressurization, Thermal Effects, Variable Fuel Properties

1. INTRODUCTION
1.1 Background and motivation
Increasingly stringent emission legislations coupled with the need to reduce the consumption of fossil fuels is driving the development of combustion engines and their sub-systems. With legislations such as Euro VI, EPA10, J-PNLT and Stage IV/Tier 4 emission requirements to fulfil, the demands on the fuel injection system are becoming more severe and increasingly higher injection pressure and system flexibility are being requested. Modern high pressure fuel injection equipment (FIE) incorporate reduced diameter injection holes that promote atomisation and reduce PM emissions. There are different routes to fulfil the NOx emission legislations for Diesel engines, based upon cooled Exhaust Gas Recirculation (EGR) and/or Selective Catalytic Reduction (SCR) (for example, [1] selectively). In combination with EGR, the effect of injection pressure on NOx is reduced, while the effect on soot emissions is maintained, as recently reported in studies from a single-cylinder Diesel engine [1]. Increasing the injection pressure to 2200bar would give engine soot out emissions suitable for Euro VI applications using a passive Diesel particulate filter (DPF), which has benefits of lower exhaust back pressure and fuel usage, thus higher engine efficiency. Further increase of injection pressure up to 2500/3000 bar is expected to put less demand on the aftertreatment systems and result to overall cheaper solution for the whole powertrain. However, increased pressure and multiple injections make the FIE sensitive and vulnerable to cavitation erosion damage [2, 3]. As a result, more accuracy is also needed to the predictive tools employed for the design of such systems.

Cavitation is known to take place inside common-rail Diesel fuel injectors that feature injection hole sizes of the order of 0.15mm or even smaller. Before entering into these discharge holes, the flow has to turn sharply from the needle seat area into the sac volume and the injection holes, giving rise to the formation of complex vortical structures. Under those flow conditions, cavitation is formed, which affects the nozzle efficiency and the subsequent spray development. For this reason a number of studies have concentrated on both experiments and calculations in an attempt to gain better understanding of this phenomenon and its effects

on the performance and durability of fuel injection systems. Due to the difficulty in obtaining real-time measurements during the injection process, most of the experimental studies reported refer to experimental devices emulating operating conditions similar to those of Diesel engines. Therefore, development and use of computational fluid dynamics models predicting cavitation seem to be the only route for obtaining information for the details of the nozzle flow under realistic operating conditions.

1.1 Fuel pressurisation effects in fuel injector nozzles and the present contribution

Irrespectively of the approach employed to simulate cavitation, the effect of variable liquid fuel properties caused by the extreme fuel pressurisation and the resulting heating are usually ignored in cavitation simulation models; moreover, the wall friction caused by liquid/wall friction within the injection hole micro-channels is also typically ignored. However, the increase of pressure is known to affect density, viscosity, heat capacity and thermal conductivity. The present study aims to assess the predictive capability of a Lagrangian cavitation model that considers the aforementioned effects in the solved conservation equations. In order to understand the effect of each variable separately, various flow simulations have been performed using two different nozzle geometries. The first one represents a fully cavitating nozzle with cylindrical hole nozzles and the second is a high-efficiency nozzle with converging tapered hole, also featuring a hole entry rounding. Combinations regarding constant or variable fuel properties with or without considering the wall friction effects of the fuel heating have been also considered.

The next paragraph describes the key assumptions and applicability limits of variable fuel properties model and the modifications introduced in the solved conservation equations without a very detailed documentation of the mathematical models, which can be found in the references quoted. Then, the results from the parametric studies are described, followed by a summary of the most important conclusions.

2. CAVITATION MODEL DESCRIPTION

A number of numerical models have appeared in the literature simulating the formation and development of cavitation inside Diesel injector nozzle [4-12]. The most promising ones are based on the assumption that cavitation is a mechanically driven phenomenon initiated by the presence of cavitation nuclei which grow to become bubbles and then to form the complex two-phase flow structures observed macroscopically in studies employing transparent nozzle (selectively [2, 13-27]). Starting from this basic assumption, the transport of vapour can be treated either as a continuous cloud, and thus simulated on an Eulerian frame of reference, or as discrete vapour/air bubbles which are tracked using an Eulerian-Lagrangian approximation. In a recent study presented in [28], it has been concluded that the Lagrangian cavitation model offers advantages compared to the Eulerian ones, since more physical processes taking place at the sub-grid scale are considered. The cavitation model used in the present study treats fuel vapor as discrete bubbles whose trajectory is calculated on a Lagrangian frame of reference. Detailed mathematical documentation of the model and extensive validation with experimental data can be found in [29]; nevertheless, the basic aspects of the physical sub-models and their numerical implementation are highlighted here, in order to help the reader to better understand the model fundamentals. Moreover, the extension of the current model to account for variable fuel viscosity and density is presented.

2.1 Liquid phase conservation equations

The GFS flow solver that has been developed by the author's group has been used in the present study. The continuous phase flow (i.e. the liquid) is described in the Eulerian frame of reference by the typical conservation equations, taking into account the effect of the liquid phase volume fraction α_L and the momentum exchange source term between the liquid and vapor phase. For the calculation of the vapor phase volume fraction, a methodology has been developed allowing for the effect of bubbles larger than the occupying cell to be taken into account accurately. This has been feasible by scanning all the cells in the vicinity of the bubble and by calculating a weighted volume contribution to all these cells. Additionally to the aforementioned conservation equations, different variations of the conventional two-equation k-ε model have been used to simulate the effects of turbulence. It has to be mentioned that in the continuity equation there is no mass source term appearing because the latent mass arising from bubble growth and collapse is negligible, due to the large density ratio. The continuity and momentum equations are listed below:

$$\frac{\partial}{\partial t}(\alpha_L \rho_L) + \nabla \cdot (\alpha_L \rho_L \vec{u}_L) = 0 \tag{1}$$

$$\frac{\partial}{\partial t}(\alpha_L \rho_L \vec{u}_L) + \nabla \cdot (\alpha_L (\rho_L \vec{u}_L \otimes \vec{u}_L - \overline{T})) = \vec{S}_{mom} \tag{2}$$

where the stress tensor is:

$$\overline{T} = -\left(p + \frac{2}{3}\mu_{eff}\nabla \cdot \vec{u}_L \right)\overline{I} + \mu_{eff}\left(\nabla \otimes \vec{u}_L + (\nabla \otimes \vec{u}_L)^T \right) \tag{3}$$

$$\mu_{eff} = \mu_L + \mu_t \tag{4}$$

In the above equation p is the pressure, $\overline{I}$ is the unit tensor μ_{eff} is the effective viscosity, calculated as the sum of the liquid dynamic viscosity μ_L and the turbulent eddy viscosity μ_t which is calculated from the local turbulent kinetic energy k and its dissipation ε. The momentum source term $\vec{S}_{mom}$ in equation (2) is evaluated by taking into account the effect of contact forces exerted upon the bubbles and of local pressure gradients. The most general form of the enthalpy equation can be written as:

$$\frac{\partial}{\partial t}(\alpha_L \rho_L h_L) + \nabla \cdot (\alpha_L \vec{u}_L(\rho_L h_L - p)) = \frac{\partial}{\partial t}(\alpha_L p) - \nabla \cdot (\alpha_L k_{eff}\nabla T) - p\nabla \cdot (\alpha_L \vec{u}_L) - G \tag{5}$$

$$k_{eff} = k_L + c_p \frac{\mu_t}{\sigma_t} \qquad \sigma_t = 0.85$$

where k_{eff} the effective thermal conductivity, calculated as the sum of the thermal conductivity k_L and the turbulent thermal conductivity $c_p \frac{\mu_t}{\sigma_t}$. G is the viscous heat production given from:

$$G = \nabla \left(\alpha_L \overline{\overline{\tau}}_{eff} \cdot \vec{u}_L \right) = \mu_t \nabla (\alpha_L \vec{u}_L) \cdot \left(\nabla \vec{u}_L + (\nabla \vec{u}_L)^T \right) - \frac{2}{3}\nabla (\alpha_L \vec{u}_L)(\rho_L k + \mu_t \nabla \vec{u}_L) \tag{6}$$

Enthalpy h is defined as:

$$dh = \left(\frac{\partial h}{\partial T} \right)_p dT + \left(\frac{\partial h}{\partial p} \right)_T dp = c_p dT + \left(\frac{\partial h}{\partial p} \right)_T dp \tag{7}$$

where T is the temperature, c_p is the specific heat under constant pressure, h_0 is the enthalpy at reference pressure p_0 and temperature T_0. For incompressible flow with constant c_p the enthalpy equation reduces to:

$$\frac{\partial}{\partial t}(\alpha_L \rho c_p T) + \nabla \cdot (\alpha_L \rho \vec{u} c_p T) = -\nabla \cdot (\alpha_L k_{eff}\nabla T) - G \tag{8}$$

A general enthalpy equation, after some rearrangements, convenient for numerical treatment with variable properties, is:

$$\frac{\partial}{\partial t}\left(\alpha_L \rho_L \overline{c}_{pmT} T \right) + \nabla \cdot \left(\alpha_L \rho_L \vec{u}_L \overline{c}_{pmT} T \right) = \frac{\partial}{\partial t}(\alpha_L p) + \vec{u}_L \cdot \nabla (\alpha_L p)$$
$$- \left(\frac{\partial (\alpha_L \rho_L h^*)}{\partial t} + \nabla \cdot (\alpha_L \rho_L \vec{u}_L h^*) \right) - \nabla \cdot (\alpha_L k_{eff}\nabla T) \tag{9}$$

where $\overline{c}_{pmT}$ is the mean c_p between T and T_0 (the reference temperature) for constant pressure p:

$$\overline{c}_{pmT} = \frac{\int_{T_0}^{T} c_p \, dT}{T - T_0} \tag{10}$$

and h* is defined as:

$$h^* = \int_{P_0}^{P} \left(\frac{\partial h}{\partial p} \right)_{T_0} dp \tag{11}$$

Correlations for both c_p and h* can be found in [30]. As a final remark regarding the above method, it ought to be mentioned that in incompressible flows the derived pressure equation is diffusive in nature; however, in

compressible flows due to the above presented density correction the final pressure equation has both convective and diffusive terms. Therefore, for the discretisation of the convective term interpolation is needed; in the current study the UPWIND scheme has been used for the interpolation of pressure in the discretised form of the continuity equation. The 1st order implicit Euler discretisation scheme has been employed for modelling the time derivatives of the solved equations. Regarding spatial discretisation, the 2nd order Jasac scheme been used.

2.2 Equations of state for variable fuel properties

In order to account for the effect of pressure and temperature on fuel properties, appropriate equations of state have to be considered. For the current study the equations of state derived in [30] have been used; the variation of density, viscosity, heat capacity and thermal conductivity for a wide range of range of pressure, for different temperatures are shown in Figure 1 for a fuel considered representative of Diesel. The pressure range considered was from atmospheric up to 2400 bar; the temperature was valid in the range from 20 to 120°C; extrapolations have been used for temperature values outside this range.
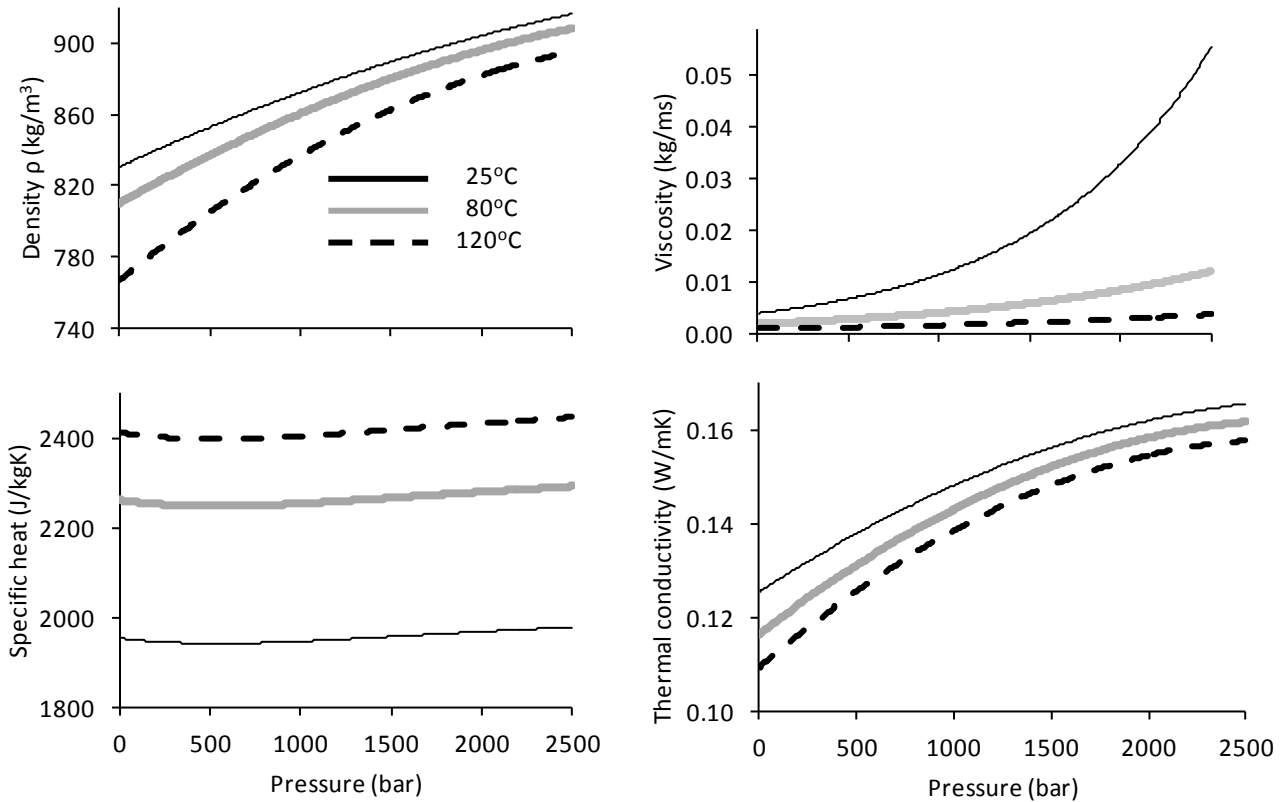

Figure 1: Fuel properties as function of pressure for three nominal temperatures

Clearly, rising pressure causes considerable variations to all properties. Density changes up to 15% while viscosity increases an order of magnitude for the lower temperature case; however, as temperature increases, variations in viscosity become smaller. Interestingly enough, heat capacity is mainly a function of fuel temperature rather than fuel pressure and increases significantly (more that 20% for a temperature increase of approximately 100^{0}C. Finally, thermal conductivity is a strong function of fuel pressure; the variation indicates that the heat conduction within the flowing liquid will be enhanced as pressure increases. During the flow simulations, the fuel properties are variables calculated as function of local pressure and temperature. The integral effect of the variation of each one of these properties on the nozzle efficiency will be presented later on as part of the parametric studies performed.

2.3 Lagrangian cavitation bubbles sub-models

Cavitation is assumed to be initiated by pre-existing nuclei present within the bulk of the flowing fluid, which subsequently grow into bubbles. These bubbles undergo various physical processes, which are taken into account utilizing a stochastic Monte-Carlo approximation: bubble parcels are used to simulate the whole population of actual bubbles, which typically count more than a few million during an injection event. These parcels are assumed to contain a number of non-interacting bubbles, which have the same size and velocity and experience the same physical processes. Many of the fundamental physical processes assumed to take place in cavitating flows are incorporated into the model. These include bubble formation through homogeneous nucleation, momentum exchange between the bubbly and the carrier liquid phase, bubble growth and collapse due to non-linear dynamics according to the early study of [31], bubble turbulent

dispersion as proposed by [32] and bubble turbulent/hydrodynamic break-up, based on the experimental observations of [33]. The effect of bubble coalescence and bubble-to-bubble interaction on the momentum exchange and during bubble growth/collapse is also considered. More details and a thorough validation of the model can be found in [28, 34]. The time step used for the simulation of the nozzle volume flow has been varied between 10^{-6}s, which is short enough to capture the transient development of the vortices formed inside the nozzle. However, a much shorter time step of 10^{-8} s has been used for simulating the cavitation structures formed inside the injection hole; it has to be noted that an adaptive time step with values down to 10^{-12} s is used in the integration of the Rayleigh-Plesset equation proposed by [35], for simulating the growth and collapse of the cavitation bubbles. The cavitation model has an inherent transient characteristic and thus transient simulations are performed even for fixed needle lift and steady pressure boundary conditions. This is due to the nature of cavitation formation and collapse processes which deviate from thermodynamic equilibrium conditions. Cavitation is initiated when the predicted pressure falls below the vapour pressure of the working fluid. When the 2nd vapour (bubbly) phase is introduced into the system of the solved equations, the pressure recovers from the values below the vapour pressure which obviously are a prerequisite for the incipience of cavitation, towards the threshold limit above which nucleation of new bubbles stops. The number of bubbles forming depends on the liquid available locally for nucleation. This result in an inherently transient pattern to the formation of bubbles since when more vapour is present, the local pressure recovers towards the nucleation threshold value, which in turn, reduces the amount of cavitation formed. This adds to the time-dependent and explosive growth/collapse process which the bubbles undergo once they have been formed.

It ought to be mentioned that direct experimental validation of the developed methodology is difficult to be performed, as point measurements (for example LDV or other laser diagnostics) is almost impossible to be performed for the actual operating conditions. However, the model has been thoroughly validated against experimental data obtained at lower injection pressures in real-size transparent Diesel injectors as well as in enlarged transparent nozzle replicas; more details can be found in [28, 36].

3. TEST CASES
Two nozzles have been utilized for the purposes of the present investigation: one with sharp inlet and cylindrical holes, referred to as 'low Cd nozzle' here after, and one with inlet rounding and tapered holes, that will be referred to as 'high Cd nozzle'. The numerical grid employed is shown in Figure 2; it consists of approximately 500,000 cells. For the purposes of the present investigation, a fixed needle lift position has been used, which correspond to that a typical nominal full lift of a production fuel injector (0.3mm).
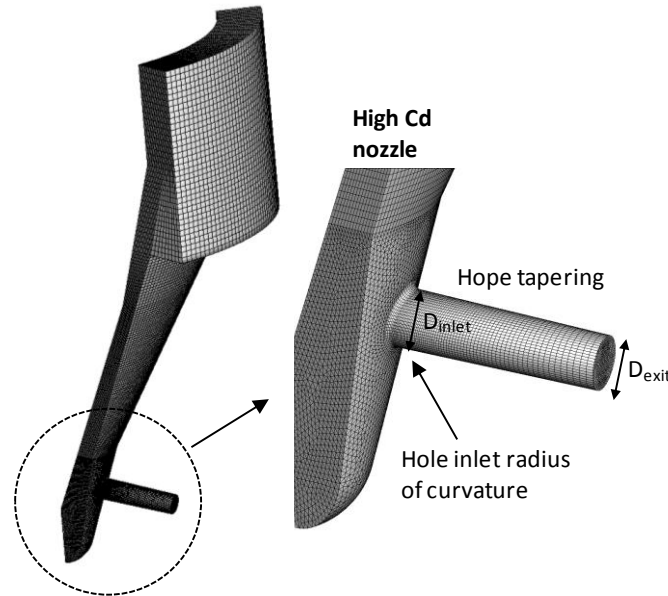

Figure 2: Numerical grid of the 60degrees sector of Diesel nozzle simulated; the *high Cd nozzle* features a curved hole inlet and hole tapering while the *low Cd nozzle* has a sharp hole inlet and cylindrical holes

The test cases simulated are listed in Tables 1 and 2 for the high and the low Cd nozzles, respectively. As the purpose here is to compare the results between the solutions obtained using fixed properties under isothermal conditions (incompressible fluid), which is the most commonly adopted assumption in such simulation reported in the literature, with those obtained using variable properties, being function of local pressure and temperature, a number of simulations cases have been performed. In addition, the effect of temperature change as a result of fuel pressurization/depressurization has been also examined. Moreover,

the effect of viscous heating has been considered by employing (a) adiabatic walls and (b) the heat transfer between the flowing liquid and the walls. With regards to influence of fuel properties, the effects of varying the density, viscosity, thermal conductivity and heat capacity have been considered. For the isothermal cases, properties have been taken at a representative temperature of 80^0C; the same value has been considered as the input temperature for the non-isothermal cases. Injection pressure has been considered fixed at 2400bar while at the downstream boundary (hole exit), a fixed pressure of 60bar has been adopted as a typical value during the injection period in turbocharged Diesel engines.

Case	Isothermal	Property variation	Viscous heating	Heat transfer
1	Yes	fixed	-	-
2	Yes	ρ, μ_l	-	-
3	Variable	ρ, μ_l, c_p, k	-	-
4	Variable	μ_l	-	-
5	Variable	ρ	-	-
6	Variable	ρ, μ_l, c_p, k	Yes	-
7	Variable	μ_l	Yes	-
8	Variable	ρ	Yes	-
9	Variable	ρ, μ_l, c_p, k	Yes	Yes

Table 1: Test cases investigated for the high Cd nozzle.

Case	Isothermal	Property variation	Viscous heating	Heat transfer
10	Yes	fixed	-	-
11	Yes	ρ, μ_l	-	-
12	Variable	ρ, μ_l, c_p, k	-	-
13	Variable	ρ, μ_l, c_p, k	Yes	-

Table 2: Test cases investigated for the low Cd nozzle.

4. RESULTS AND DISCUSSION
In this section the results obtained are presented. These are divided into three sub-sections. Initially, we report estimates of the mean temperature change through similar micro-channels utilizing a zero-dimensional energy equation balance. Then, results from the 3-D flow distribution are presented, followed by estimates of the % variation of the mass injected and mean fuel temperature increase at the nozzle hole exit for the above listed test cases.

4.1 Zero-dimensional energy balance
As the flow is accelerated within the injection hole, the liquid pressure is converted mostly into fuel kinetic energy but inevitably some losses also occur. The nozzle discharge coefficient is defined as the ration between the actual mass injected over that calculated by the Bernoulli equation. Assuming that the imbalance between the potential energy and the kinetic energy is converted into heat (turbulent kinetic energy is neglected) and utilizing the above relations for the Diesel properties, we can estimate the expected mean temperature increase of the fuel as function of the nozzle discharge coefficient; this relation is shown in Figure 3. Two lines are plotted, one corresponding to estimates obtained with fixed density and one with variable density as function of pressure and temperature. The shaded areas superimposed on top of this figure indicate the range of expected Cd values for typical Diesel injector nozzles as those considered later on for the 3-D analysis. In addition, the Cd values corresponding to very low needle lifts (partial needle opening) are also indicated. These estimates have been obtained assuming an initial fuel temperature of 80^oC. These estimates predict that despite fuel depressurization that causes fuel acceleration inside the

injection hole, temperature also increases, particularly for the partial needle opening case of for the low Cd nozzle. Interestingly enough, liquid compressibility compensates some of the expected fuel heating while some cooling is predicted for the compressible case for Cd values close to 1. The observed temperature increase occurring with decreasing nozzle discharge coefficient may result to boiling in certain locations as opposed to cavitation; such phase-change effects initiating from the surface of the metallic nozzle have not considered in the 3-D computational model that is presented in the following section.
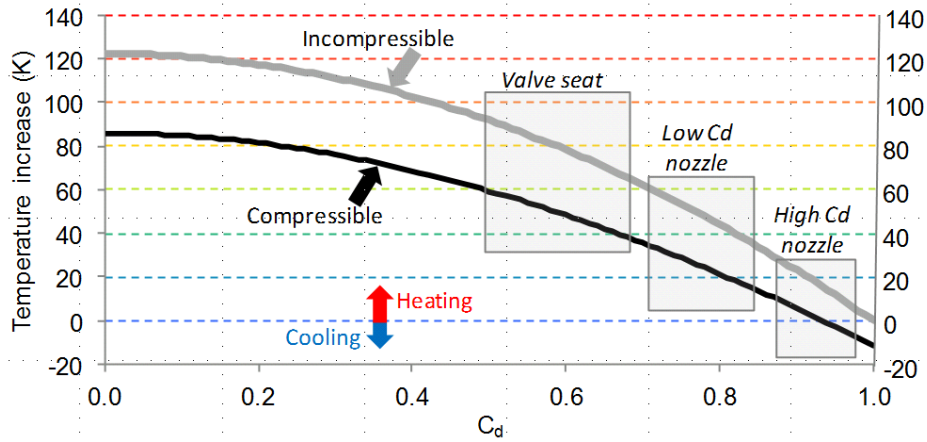

Figure 3: Diesel temperature increase as function of the discharge coefficient of the flow passage

4.2 Flow distribution from 3-D simulation

In this section results from the 3-D flow simulations are presented. Initially, an overview of the flow pattern is given followed by more detailed comparison of the effects captured from the cases of Tables 1 and 2. Figures 4a and 4b show the flow path lines inside both the low and the high Cd nozzles, respectively. The flow structure is similar within the sac volume for both designs; a large vortex forming just below the bottom part of the injection hole can be observed. At the upper part of the injection hole, two counter rotating vortices are formed, which are much stronger in the case of the low Cd nozzle. The pressure distribution is also depicted on the contour plot passing through the symmetry plane of the injection hole. It is clear that pressure follows a rather different pattern between the two designs. In the cylindrical nozzle, the pressure drops as the flow enters into the injection hole with the cavitation formation area extending almost down to half of the injection hole length. On the contrary, in the tapered nozzle, cavitation is forming only at the top part of the injection hole which is also highlighted in order to become better visible. Around and below that vapor formation pocket, the pressure is well above the threshold value for cavitation initiation while drops gradually towards the pressure value imposed as boundary condition at the nozzle hole exit plane; this is typical for holes having a converging tapered shape towards the hole exit. As differences attributed to variation of fuel properties cannot become visible using this color scale, they are presented in detail in the following paragraphs.
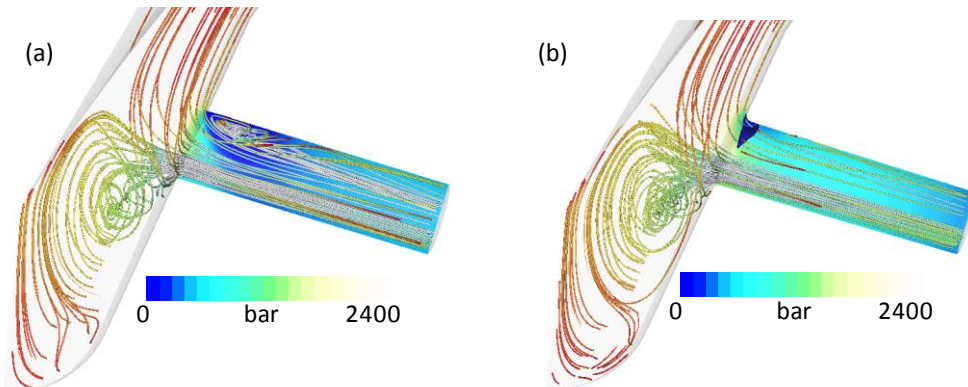

Figure 4: Flow distribution within the injection nozzles investigated; (a) low Cd nozzle and (b) high Cd nozzle

The following Figure 5 shows the predicted temperature distribution on the surface of the two nozzle designs considered. It has to be mentioned that the nozzle wall temperature during normal Diesel engine operation should not exceed 230^{0}C, which is much higher than the 80^{0}C of the fuel inlet temperature assumed in the simulations performed here. The results indicate that despite the fuel depressurisation and the reduction in density from the hole inlet to the hole exit, which can be seen in Figure 6, a significant temperature increase due to wall friction occurs. This can exceed locally 60-80^{0}C relative to the fuel inlet temperature for this

particular operating condition and nozzle designs investigated. Overall, more heating and relatively more uniform temperature distribution can be observed on the low Cd nozzle design.
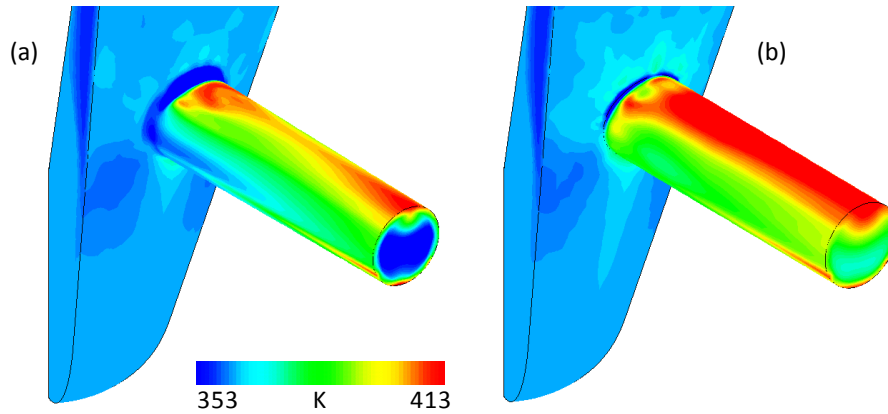

Figure 5: Predicted temperature distribution on the nozzle wall surface for the (a) high Cd [*Case 6, Table 1*] and (b) low Cd nozzles [*Case 13, Table 2*] as predicted when viscous heating is considered
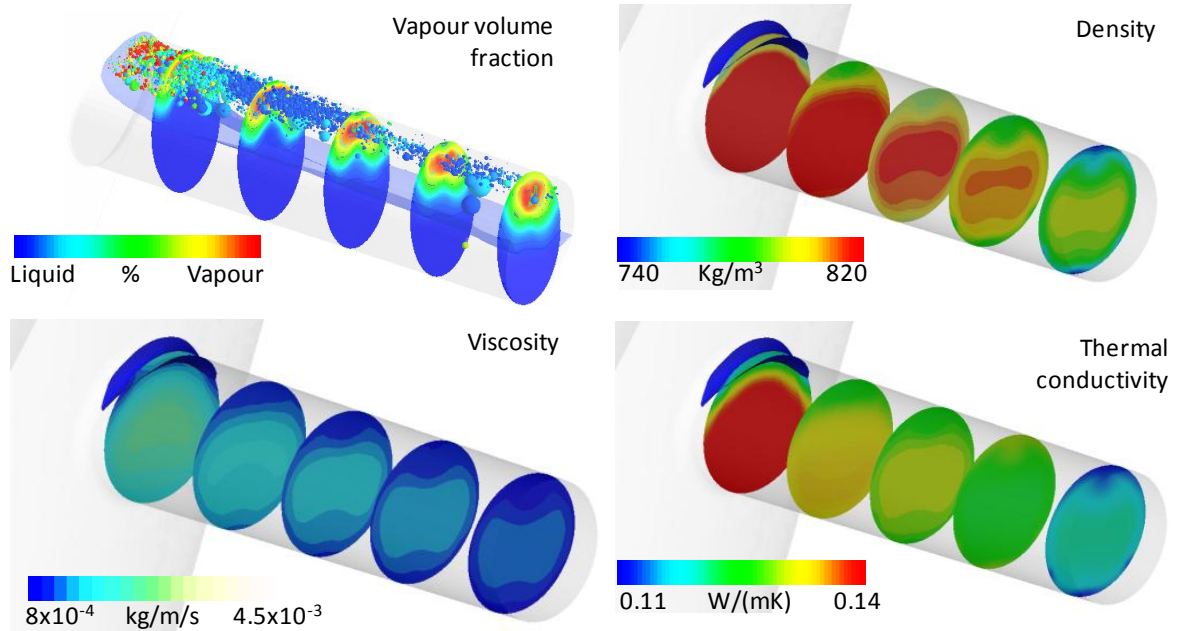

Figure 6: Predicted vapour volume fraction, density, viscosity and thermal conductivity distributions [*Case 9, Table 1*]

Figure 6 shows the distribution of vapour volume fraction (with sample cavitation bubbles superimposed), density, viscosity and thermal conductivity on 5 cross sections normal to the injection hole axis from the inlet to the exit; for these contours, the data set of Case 9 from Table 1 has been used, which considers the variation of all properties, the viscous heating produced by wall friction and adiabatic walls. Fuel viscosity decreases as it follows mainly the pressure distribution along the injection hole. Thermal conductivity also decreases, which implies decreased diffusion of the heat produced from the wall friction within the bulk of the liquid; this will enhance temperature gradients in the radial direction across the hole sectional area towards the hole exit.

4.3 Integral effect on fuel injection quantity and mean injection temperature
Following the presentation of the flow distribution within the sac volume and the nozzle hole, it has been considered useful to examine in more detail the variation of the injected mass and the temperature difference from the inlet relative to that of the reference cases; these are Case 1 and Case 10 for the high and the low Cd nozzles, respectively. Figure 7 summarizes these results for both nozzles and for all cases investigated.
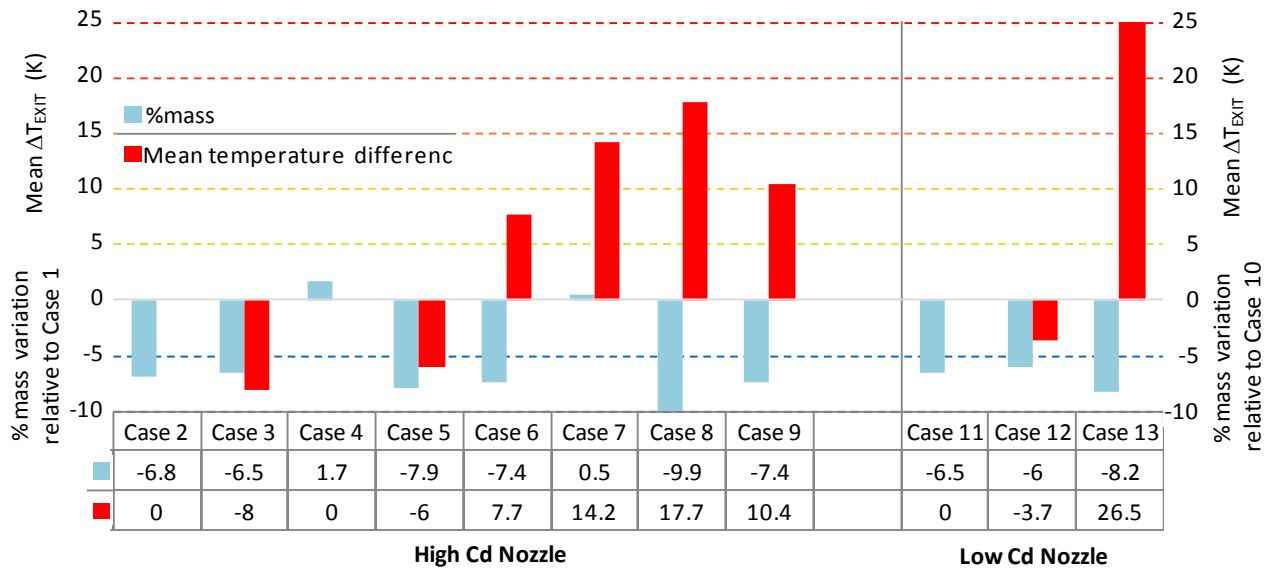
The chart shows two y-axes labeled "Mean ΔT$_{EXIT}$ (K)" (top) and "% mass variation relative to Case 1" / "% mass variation relative to Case 10" (bottom), with values from 25 down to -10.

	Case 2	Case 3	Case 4	Case 5	Case 6	Case 7	Case 8	Case 9		Case 11	Case 12	Case 13
%mass	-6.8	-6.5	1.7	-7.9	-7.4	0.5	-9.9	-7.4		-6.5	-6	-8.2
Mean temperature difference	0	-8	0	-6	7.7	14.2	17.7	10.4		0	-3.7	26.5

High Cd Nozzle   **Low Cd Nozzle**

Figure 7: Predicted % mass flow rate difference and mean temperature difference at the nozzle exit relative to the reference case for the conditions of Tables 1 and 2

It is interesting to notice that when viscous heating is ignored, a reduction in the mean fuel temperature is predicted relative to the isothermal case, which is a result of the fuel depressurization. Still, this temperature drop, which is less than 10 degrees for the particular cases investigated here, is significantly smaller that the corresponding temperature increase caused by the fuel pressurization to the rail pressure level, as this process is not reversible. When viscous heating is calculated, then the mean fuel exit temperature can increase up to 25^{0}C for the case of the more cavitating low Cd nozzle relative to the incompressible (and isothermal) case. Concentrating to the variation of fuel viscosity only (cases 4 and 7), it can be seen that this results to a small increase (rather than decrease as observed in all other cases) in fuel injection quantity relative to the incompressible reference case 1. This implies that for the given range of variation, the heat produced results to reduced viscosity and less losses overall. Moreover, comparison of the temperature increase between cases 6 and 9 reveals the effect of wall heat transfer. This comparison indicates that heat transfer does not result to excess fuel heating relative to that produced through friction. It is expected that as injection pressures will increase further, the increased viscous heating may result to near-wall temperatures very close or even higher to those of the heated from the combustion chamber nozzle wall metal. Finally, comparison between the high and the low Cd nozzles, indicates that the most cavitating nozzle results to much higher temperature increase, as this is associated with more pressure losses within the nozzle hole. With regards to the fuel injection quantity, it is clear that when variable fuel properties and heating effects are considered, a significant reduction is recorded relative to the incompressible case. This variation is of the order of 5-10% for both nozzle designs. It ought to be mentioned that the calculated reduction of the injected mass due to cavitation is approximately 10-12% for the high Cd nozzle when incompressible fluid is assumed. Thus, the influence of the parameters considered here are comparable to those caused by considering cavitation.

CONCLUSIONS

The GFS three dimensional RANS CFD flow solver that incorporates a Eulerian-Lagrangian cavitation model has been used to investigate the effect of variable fuel properties and wall friction on the cavitation characteristics, volumetric efficiency and temperature increase in two typical mini-sac Diesel injector designs; these designs correspond to a fully cavitating one that has been referred to as *low Cd nozzle* and one that features inlet hole rounding and hole tapering that suppress cavitation and result to *higher Cd* values. Variable fuel properties have been taken from appropriate equations of state for Diesel fuel. In addition to the mass and momentum conservation equations, the energy equation that accounts viscous heating and the terms associated with variable density, viscosity, heat capacity and thermal conductivity have been considered and implemented in the solved equations. Moreover, the presence of the cavitation vapour phase is taken into account while a number of sub-grid scale physical models have been employed for capturing the formation and further development of cavitation.

The results indicate that the energy losses occurring within the injection hole can induce fuel heating. Wall friction can induce temperatures substantially higher than the bulk liquid temperature which can be well above the boiling point of the fuel. When variable fuel properties are considered, a substantial reduction in the volumetric efficiency of the nozzle is predicted relative to that of the incompressible case. It can thus be

concluded that computational models employed to assist in the design of modern Diesel fuel injector, expected to operate in excess of 2500bar, should consider thermal and variable fluid properties effects.

REFERENCES

1. Daum S, Gill D, and Theissl H, *Medium and heavy duty diesel fuel injection system requirements to meet future emissions legislation.* IMechE Conference on Fuel Injection Systems for IC Engines, London, 2012.
2. Gavaises, M., *Flow in valve covered orifice nozzles with cylindrical and tapered holes and link to cavitation erosion and engine exhaust emissions.* International Journal of Engine Research, 2008. **9**(6): p. 435-447.
3. Gavaises, M., et al. *Link Between Cavitation Development and Erosion Damage in Diesel Injector Nozzles.* in *SAE 2007-01-0246.* 2007.
4. Kubota, A., H. Kato, and H. Yamaguchi, *A New Modelling of Cavitating Flows - a Numerical Study of Unsteady Cavitation on a Hydrofoil Section.* Journal of Fluid Mechanics, 1992. **240**: p. 59-96.
5. Avva, R.K., A. Singhal, and D.H. Gibson. *An Enthalpy Based Model of Cavitation.* in *Cavitation and Multiphase Flow Forum, ASME FED.* 1995.
6. Schmidt, D.P., C.J. Rutland, and M.L. Corradini, *A Numerical Study of Cavitating Flow Through Various Nozzle Shapes.* SAE Paper 971597, 1997.
7. Grogger, H.A. and A. Alajbegovic. *Calculation of the Cavitating Flow in Venturi Geometries using Two Fluid Model.* in *Proc. of FEDSM'98 - 1998 ASME Fluid Engineering Division Summer Meeting.* 1998. Washington, D.C., USA.
8. Yuan, W., J. Sauer, and G.H. Schnerr. *Modeling and Computation of Unsteady Cavitation Flows in Injection Nozzles.* in *1st International Colloquium on Microhydrodynamics.* 2000. Paris, France.
9. Marcer, R., et al., *A Validated Numerical Simulation of Diesel Injector Flow Using a VOF Method.* SAE Paper 2000-01-2932, 2000.
10. Singhal, A.K., et al. *Mathematical basis and validation of the full cavitation model.* in *Proc. of FEDSM'01 - 2001 ASME Fluid Engineering Division Summer Meeting.* 2001. New Orleans, Louisiana, USA.
11. Singhal, A.K., et al., *Mathematical basis and validation of the full cavitation model.* Journal of Fluids Engineering-Transactions of the ASME, 2002. **124**(3): p. 617-624.
12. Giannadakis, E., et al. *Cavitation Modelling in Single-Hole Diesel Injector Based on Eulerian-Lagrangian Approach.* in *Proc. THIESEL International Conference on Thermo- and Fluid Dynamic Processes in Diesel Engines.* 2004. Valencia, Spain.
13. Arcoumanis, C., et al., *Cavitation in Real-Size Multi-Hole Diesel Injector Nozzles.* SAE Transactions, Journal of Engines, 2000-01-1249, 2000. **109-3**.
14. Afzal, H., et al., *Internal flow in diesel injector nozzles: modelling and experiments.* IMechE Paper S, 1999. **492**: p. 25-44.
15. Arcoumanis, C., et al., *Visualisation of cavitation in diesel engine injectors.* Mécanique & industries, 2001. **2**(5): p. 375-381.
16. Badock, C., et al., *Investigation of cavitation in real size diesel injection nozzles.* Int. Journal of Heat and Fluid Flow, 1999. **20**(5): p. 538-544.
17. Blessing, M., et al., *Analysis of Flow and Cavitation Phenomena in Diesel Injection Nozzles and its Effect on Spray and Mixture Formation.* SAE Technical Paper 2003-01-1358, 2003.
18. Chaves, H., et al., *Experimental Study of Cavitation in the Nozzle Hole of Diesel Injectors Using Transparent Nozzles.* SAE Technical Paper 950290, 1995.
19. Gavaises, M., et al., *Characterization of string cavitation in large-scale Diesel nozzles with tapered holes.* Physics of Fluids, 2009. **21**(5): p. 052107.
20. Gavaises, M., et al., *Link Between Cavitation Development and Erosion Damage in Diesel Injector Nozzles.* SAE Technical Paper 2007-01-0246, 2007.
21. Lockett, R.D., et al., *The characterisation of diesel cavitating flow using time-resolved light scattering.* IMechE Conf. in Fuel Systems, London, 2009.
22. Mitroglou, N., M. Gavaises, and C. Arcoumanis. *Spray stability from VCO and a new Diesel nozzle design concept.* in *IMechE Conf. in Fuel Systems, London.* 2012.
23. Reid, B.A., Hargrave G.K, Garner C.P, Long E. J and Khoo Y.C *An Investigation of Internal Flow Structures in Real-Sized High-Pressure Fuel Injectors.* in *8th Int. Symp. on PIV, Paper No 0132.* 2009. Melbourne, Australia.
24. Roth, H., M. Gavaises, and C. Arcoumanis, *Cavitation Initiation, Its Development and Link with Flow Turbulence in Diesel Injector Nozzles.* SAE Transactions Journal of Engines, 2002-01-0214, 2002. **111-3**: p. 561-580.
25. Roth, H., et al., *Effect of multi-injection strategy on cavitation development in diesel injector nozzle holes.* SAE transactions, 2005. **114**(3): p. 1029-1045.
26. Soteriou, C., R. Andrews, and M. Smith, *Direct Injection Diesel Sprays and the Effect of Cavitation and Hydraulic Flip on Atomization.* SAE Technical Paper 950080, 1995.

27. Soteriou, C., et al. *The flow characteristics of high efficiency Diesel nozzles with enhanced geometry holes.* in *THIESEL Int. Conf. on Thermo- and Fluid Dynamic Processes in Diesel Engines.* 2006. Valencia, Spain.

28. Giannadakis, E., et al., *Evaluation of the predictive capability of diesel nozzle cavitation models.* SAE Paper 2007-01-0245, 2007.

29. Giannadakis, E., M. Gavaises, and C. Arcoumanis, *Modelling of Cavitation in Diesel Injector Nozzles.* accepted in Journal of Fluid Mechanics, 2008.

30. Kolev, N., *Multiphase Flow Dynamics 3: Turbulence, Gas Absorption and Release, Diesel Fuel Properties.* 2002: Springer Verlag Berlin Heidelberg.

31. Prosperetti, A. and M.S. Plesset, *Vapour-bubble growth in a superheated liquid.* Journal of Fluid Mechanics, 1978. **85**(2): p. 349-368.

32. Farrell, K.J., *Eulerian/Lagrangian analysis for the prediction of cavitation inception.* Journal of Fluids Engineering-Transactions of the ASME, 2003. **125**(1): p. 46-52.

33. Martínez-Bazán, C., J.L. Montañés, and J.C. Lasheras, *On the breakup of an air bubble injected into a fully developed turbulent flow. Part 2. Size PDF of the resulting daughter bubbles.* Journal of Fluid Mechanics, 1999. **401**: p. 183-207.

34. Giannadakis, E., *Modelling of Cavitation in Automotive Fuel Injector Nozzles.* 2005, PhD Thesis, Imperial College, University of London.

35. Plesset, M.S. and A. Prosperetti, *Bubble Dynamics and Cavitation.* Annual Review of Fluid Mechanics, 1977. **9**: p. 145-185.

36. Giannadakis, E., M. Gavaises, and C. Arcoumanis, *Modelling of cavitation in diesel injector nozzles.* Journal of Fluid Mechanics, 2008. **616**(1): p. 153-193.